



Synthesis and Photochemical Properties of 2,3;5,6-bis(cyclohexano)-BODIPY

Anna Yu. Kritskaya¹ · Natalia A. Bumagina¹ · Elena V. Antina¹ · Alexander A. Ksenofontov¹  · Mikhail B. Berezin¹ · Alexander S. Semeikin²

Received: 23 August 2017 / Accepted: 7 December 2017
© Springer Science+Business Media, LLC, part of Springer Nature 2017

Abstract

The boron-dipyrromethene (BODIPY) dye containing an annelated cyclohexyl rings at the 2,3 and 5,6-positions of pyrroles has been synthesized and characterized. Photochemical properties of the obtained compound have been investigated in different individual solvents. 2,3;5,6-Bis(cyclohexano)-BODIPY exhibits intense chromophore properties with maximum of $S_0 \rightarrow S_1$ band in the 543–549 nm (A from 66000 to 96000 L/mol·cm). The complex is a fluorophore with a quantum yield up to ~100%. The influence of solvent polarity on the spectral properties was evaluated. To better understand the spectroscopic results, quantum chemical calculations were carried out. Photostability of dye was studied.

Keywords BODIPY · Spectral properties · Solvatochromism · Photostability · Quantum chemical calculations

Introduction

At present, the family of 4,4-difluoro-4-boron-3a, 4a-diaza-s-indacene dyes of (known under the BODIPY trademark (Fig. 1a)) is the subject of active research. According to the data, presented in the review by Jorge Banuelos in 2016, the publications number devoted to chromophores of this class is increased exponentially in the past few years [1].

Interestingly, the first report about BODIPYs appeared about 50 years ago (in 1968) [2], but their unique luminescent properties at that time were not studied. As a result, over the next 20 years, these dyes did not attract the interest of scientists.

The first results, confirming the prospects of using BODIPYs as active media of tunable lasers, were appeared only in the early 1990s of the last century as a result of research by Boyer et al. [3–5]. Optimum laser performance of these dyes is due to their high chemical and thermal stability, low propensity to photodestruction and unique photo-physical properties that are more dependent on the molecular structure [6–12]. Due to the first encouraging results since the 1990s, the direction of BODIPY dyes has received special attention from the scientific community and by now has turned into several rapidly and successfully developing areas of science and technology [13–16]. The most important and intensively developing field of application of BODIPY fluorophores is sensorics (fluorescent sensors, switches and probes) [17–19], biochemical sciences (fluorescent markers for bio-recognition) [20–22], medicine (singlet-oxygen generators in photodynamic therapy) [23, 24]. BODIPYs are also promising in light-storage arrays for antenna systems [25, 26], in photovoltaics [27, 28] and other directions.

Most BODIPY chromophores are relatively well soluble in most organic solvents. The main reason for the success and universality of BODIPYs is its chromophoric core,

✉ Alexander A. Ksenofontov
ivalex.09@mail.ru

Anna Yu. Kritskaya
aynikonova@mail.ru

Natalia A. Bumagina
27angel07@mail.ru

Elena V. Antina
eva@isc-ras.ru

Mikhail B. Berezin
mbb@isc-ras.ru

Alexander S. Semeikin
semeikin@isuct.ru

¹ G.A. Krestov Institute of Solution Chemistry of Russian Academy of Sciences (ISC RAS), 1 Akademicheskaya st., 153045 Ivanovo, Russian Federation

² Ivanovo State University of Chemistry and Technology (ISUCT), 7 Sheremetevskij prosp., 153000 Ivanovo, Russian Federation

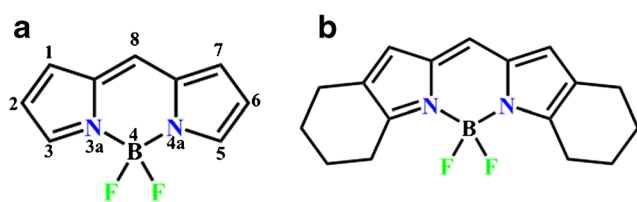
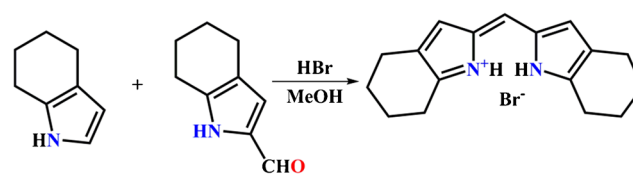


Fig. 1 Structure of BODIPY (**a**) and 2,3;5,6-bis(cyclohexano)-BODIPY **1** (**b**)

due to which their solutions are characterized by intense absorption and fluorescence in the visible and near infrared regions of the spectrum. The molar absorption coefficient at the maximum of the intense band reaches $10^5 \text{ M}^{-1} \text{ cm}^{-1}$. The fluorescence quantum yield can reach 100% and weakly depends on the properties of the environment [9, 13, 29].

The physico-chemical properties of BODIPYs can vary considerably depending on the nature of the functional substituents in their chromophore core. There are many variants of the functionalization of the dipyrromethene ligand, which makes it possible to obtain a variety of BODIPY derivatives [13, 15, 16]. The main ways of modification of the BODIPY structure include the replacement of hydrogen atoms in the 1,2,3,5,6,7,8-positions of the dipyrromethene core by different functional groups; replacement of methine *meso*-spacer by nitrogen atom; the replacement of the anion fluoride at the boron(III) atom by other ligands.

Another method is based on annelation of cyclic aromatic or aliphatic rings to the pyrrole fragments of the dipyrromethene core. Unlike BODIPY with an extended π -system [30, 31], information about BODIPYs with cyclic aliphatic substituents is extremely limited. The first data about BODIPYs with cyclic aliphatic substituents were appeared only in 2007 in a review by Loudet and Burgess [13] and the article by Thompson et al. [32]. The properties of 3-chloro-5,6-cyclohexano-BODIPY, obtained by the authors from Belgium [33], were also remained unexplored. In 2008, Liangxing Wu and Kevin Burgess in their paper [34] presented the synthesis results and characteristics of absorption and fluorescence electron spectra of 2,3;5,6-bis(cyclohexano)-BODIPY in methylene chloride. And only in 2016 I. A. Boldyrev et al. in their work described 2,3;5,6-bis(cyclohexano)-BODIPY as novel fluorescent membrane (phosphatidylcholine) probe [35]. However, photophysical properties of this complex were poorly investigated. A detailed study of the physico-chemical properties is primarily necessary to describe the prospects for the practical using new cyclohexano-BODIPYs. Therefore, in this paper for the first time



Scheme 1 Synthesis of 2,3;5,6-bis(cyclohexano)-dipyrromethene hydrobromide

we present the experimental results of the detailed investigation of the spectral-luminescent properties of 2,3;5,6-bis(cyclohexano)-BODIPY **1** (Fig. 1b) in wide range of organic solvents together with the results of ^1H NMR analysis of related compounds and the results of quantum chemical calculations (molecular structure optimization, spectroscopic characteristics and FMOs energies), and the results of analysis of the spectral characteristics depending on the solvatochromic parameters (Lippert and Dimroth-Reichardt). Additionally, photostability of complex by UV irradiation was studied.

Experimental

Materials

Propanol-1 (UV-IR-HPLC-HPLC preparative PAI) and **cyclohexane** (Panreac, Barcelona) were used without further purification. Other **solvents** were purified according to the procedures described in [36, 37].

Synthesis

2,3;5,6-Bis(cyclohexano)-dipyrromethene hydrobromide ($\text{C}_{17}\text{H}_{21}\text{N}_2\text{Br}$; M 333.27) was prepared by reacting 2,3-cyclohexanopyrrole with 2,3-cyclohexano-5-formylpyrrole in a methanol solution in the presence of hydrobromic acid according to Scheme 1.

With mixing and room temperature, the 2 ml of concentrated hydrobromic acid were added to solution of 1.8 g (14.8 mmol) of 2,3-cyclohexanopyrrole (M 121.18) and 2.01 g (13.45 mmol) of 2,3-cyclohexano-5-formylpyrrole (M 149.19) in a 20 ml of methanol (Scheme 1). The mixture was stirred for 2 h. The precipitate was filtered off, washed on the filter with water, methanol and air-dried. Yield: 14.5 mmol (89%). $\lambda_{\text{max}} = 496$; 345 nm (CH_2Cl_2). ^1H NMR spectrum (CDCl_3), δ , 13.25 s (2H, NH), 6.99 s (1H, ms-H), 6.80 s (2H, 1,7-H), 3.13 t (4H, CH_2), 2.57 t (4H, CH_2), 1.82–1.86 m

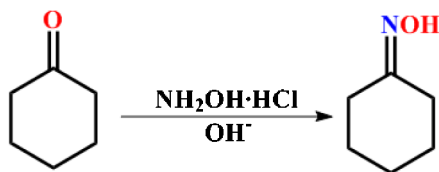
(4H, CH₂), 1.75–1.79 m (4H, CH₂). Found, %: C 61.22, H 6.24, N 8.31. C₁₇H₂₁N₂Br. Calculated, %: C 61.27, H 6.35, N 8.41.

Synthesis of 2,3;5,6-bis(cyclohexano)-dipyrromethene difluoroborate (C₁₇H₁₉BF₂N₂; *M* 300.16) was based on the exchange reaction of 2,3;5,6-bis(cyclohexano)-dipyrromethene hydrobromide with boron(III) trifluoride etherate as complexing agent (Scheme 2).

To solution of 1.87 g (5.61 mmol) of 2,3;5,6-bis(cyclohexano)-dipyrromethene hydrobromide in 50 ml of methylene chloride, the 5.67 g (56.1 mmol) of triethylamine and 7.96 g (56.1 mmol) of boron trifluoride etherate were added at room temperature and mixing (Scheme 2). The solution was kept under stirring for 2 h, then was washed with water. The solvent was distilled off, and the complex was chromatographed on silica gel (methylene chloride as eluent). The solvent was evaporated. The complex was precipitated with methanol under cooling. Yield: 0.6 g (1.99 mmol; 35.6%). λ_{max} = 547; 361 nm (CH₂Cl₂). ¹H NMR spectrum (CDCl₃), δ, 6.93 s (1H, ms-H), 6.64 s (2H, 1,7-H), 3.06 t (4H, J=6.2 Hz, CH₂), 2.57 t (4H, J=6.2 Hz, CH₂), 1.84–1.91 m (4H, CH₂), 1.73–1.80 m (4H, CH₂). ¹³C{¹H} NMR (CDCl₃), δ, 22.3, 22.8, 23.2, 24.7, 76.8, 77.0, 77.3, 125.3, 125.9, 129.3, 134.0, 158.0. ¹¹B NMR (CDCl₃): δ 0.68 (t). Found, %: C 67.93, H 6.24, N 9.18. C₁₇H₁₉N₂BF₂. Calculated, %: C 68.03, H 6.38, N 9.33. Mass spectrum MALDI-TOF: calculated (C₁₇H₁₉N₂BF₂) *m/z* = 300.16, found *m/z* = 300.1651.

The 2,3-cyclohexanopyrrole and 2,3-cyclohexano-5-formylpyrrole were prepared as follows.

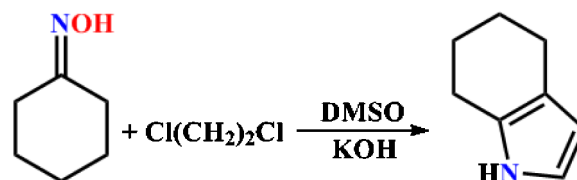
Cyclohexanone oxime (C₆H₁₁NO; *M* 113.16)



The 70 g (1.01 mol) of hydroxylamine hydrochloride (NH₂OH·HCl) in 300 ml of water was added portionwise to 98 g (103.4 ml, 1.0 mol) of cyclohexanone. Then, the KOH

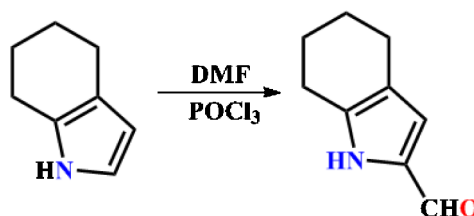
solution was added to pH = 7. The solution was cooled, the precipitate was filtered off and air-dried. Yield: 88 g (78%).

2,3-Cyclohexanopyrrole (C₈H₁₁N; *M* 121.18)



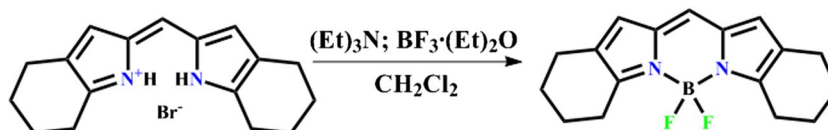
To a mixture of 95 g (1.7 mol) of KOH and 27 g (0.24 mol) of cyclohexanone oxime in 150 ml of DMSO, the 41.3 g (0.48 mol) of 1,2-dichloroethane in 38 ml of DMSO were added dropwise with stirring and heating (120 °C). The mixture was then stirred for an additional 30 min, cooled, poured into water and distilled with water vapor. The distillate was extracted with ether. The ether was distilled off, and the pyrrole was distilled under vacuum, collecting the fraction ≈ 123 °C. Yield 7 g (27%).

2,3-Cyclohexano-5-formylpyrrole (C₉H₁₁NO; *M* 149.19)



The 3.0 ml (0.032 mol) of phosphorus oxychloride was added dropwise to a solution of 2.89 g (0.024 mol) of 2,3-cyclohexanopyrrole in 18 ml of dried DMF with stirring and cooling (temperature below 20 °C). The mixture was then stirred for 1.5 h at room temperature, poured into 100 ml of water, filtered and basified to an alkaline reaction with 20% sodium hydroxide solution (~9 g of NaOH) with cooling. After a few hours, the precipitate was filtered off, washed with water and dried at room temperature. Yield 2.8 g (78%).

Scheme 2 Synthesis of 2,3;5,6-bis(cyclohexano)-BODIPY



Spectroscopy

^1H NMR, ^{13}C NMR and ^{11}B NMR (CDCl_3) spectra were carried in the centre for joint use of scientific equipment “The upper Volga region centre of physico-chemical research” on the spectrometer Bruker 500 (Germany) [38, 39].

Mass spectrum (MALDI-TOF) of 2,3;5,6-bis(cyclohexano)-BODIPY was performed on AXIMA Confidence (Shimadzu) MALDI-TOF mass spectrometer.

Electronic absorption spectra (EAS) of solutions of compound 1 were recorded on SM 2203 spectrofluorimeter (SOLAR) in the range of molar concentrations from $1 \cdot 10^{-5}$ to $2 \cdot 10^{-5}$ mol/l and thickness of absorbing layer is 10 mm at $T = 25 \pm 0.1$ °C.

Fluorescence spectra were obtained on spectrofluorimeter SM 2203 (SOLAR) at an optical density not higher than 0.1 at the excitation wavelength (495–500 nm).

Stokes shift was calculated as the difference between the values of maxima of the intense bands in the fluorescence and absorption spectra:

$$\Delta\lambda(\text{nm}) = \lambda_{\text{max}}^{\text{fl}} - \lambda_{\text{max}}^{\text{abs}} \quad \text{and} \quad \Delta\nu_{\text{st}}(\text{cm}^{-1}) = \nu_{\text{max}}^{\text{abs}} - \nu_{\text{max}}^{\text{fl}}$$

Full width at half maximum (FWHM, cm^{-1}) in the electronic absorption and fluorescence spectra was determined as the difference between the maximum and minimum values of the wavelengths, taken at half of intensity of $S_0 \rightarrow S_1$ band.

The fluorescence quantum yields (φ) of BODIPY 1 were obtained with the following equation: $\varphi_{\text{sample}} = \varphi_{\text{standard}} \cdot (S_{\text{sample}}/S_{\text{standard}}) \cdot (A_{\text{standard}}/A_{\text{sample}}) \cdot (n_{\text{sample}}/n_{\text{standard}})^2$, where S denotes the area under the fluorescence band of sample (BODIPY 1) and standard (Rhodamine 6G in ethanol with $\varphi = 94\%$ [40, 41]), A denotes the absorbance of sample and standard at the excitation wavelength, and n denotes the refractive index of the solvent.

The fluorescence lifetime (τ) was estimated based on the spectral-luminescent characteristics. In accordance with $\varphi = k_{\text{rad}}/(k_{\text{rad}} + k_{\text{nr}})$ and $\tau = 1/(k_{\text{rad}} + k_{\text{nr}})$, fluorescence lifetime was determined by: $\tau = \varphi / k_{\text{rad}}$, where k_{nr} is the rate of non-radiative processes, k_{rad} is rate of radiative processes (radiation constant). The rate constant of radiative deactivation was estimated from the characteristics of the electronic absorption spectra in accordance with the [42, 43]:

$$k_{\text{rad}} = 2.9 \cdot 10^{-9} \cdot [(9n_{\text{D}}^2)/(n_{\text{D}}^2 + 2)^2] \cdot \nu_{\text{max}}^2 \cdot A_{\text{max}} \cdot \Delta\nu_{1/2}$$

where n_{D} is the refractive index of the solvent, ν is wave number of absorption band maximum (cm^{-1}); $\Delta\nu_{1/2}$ is half-width of the absorption band (cm^{-1}); A is extinction coefficient of intense absorption band ($\text{l/mol}\cdot\text{cm}$).

The rate constant of nonradiative deactivation (k_{nr}) was calculated from experimentally measured fluorescence

quantum yield and fluorescence lifetime according to the following equations:

$$k_{\text{nr}} = (1 - \varphi)/\tau$$

The function of universal interactions (Δf), used as a solvent polarity parameter, was calculated according to the equation of Lippert (Table 1) [42]:

$$\Delta f = f(\varepsilon) - f(n_{\text{D}}^2) = \left(\frac{\varepsilon - 1}{2\varepsilon + 1} \right) - \frac{n_{\text{D}}^2 - 1}{2n_{\text{D}}^2 + 1}$$

where ε is dielectric constant, n_{D} is the refractive index of the solvent. The $f(\varepsilon)$ is total polarization and $f(n_{\text{D}}^2)$ is induction polarization.

The Dimroth-Reichardt parameter (E_{T}) takes into account the polarity and polarizability of the solvent. We used a dimensionless normalized (E_{T}^{N}) Dimroth-Reichardt parameter:

$$E_{\text{T}}^{\text{N}} = \frac{E_{\text{T}}(\text{solvent}) - E_{\text{T}}(\text{tms})}{E_{\text{T}}(\text{water}) - E_{\text{T}}(\text{tms})} = \frac{E_{\text{T}}(\text{solvent}) - 30,7}{32,4}$$

E_{T} (tms)- polarity parameter of the tetramethylsilane; E_{T} (water)- polarity parameter of the water; E_{T} (solvent)- polarity parameter of the solvent. Tetramethylsilane and water are standard solvents with extreme polarities. E_{T}^{N} varies from 0,0 (tetramethylsilane is the least polar solvent) to 1,0 (water is the most polar solvent).

Quantum Chemical Calculations

All DFT, TD-DFT theoretical calculations were performed using the PC GAMESS v.12 program package [45]. Geometry optimization of BODIPY 1 in the ground state (S_0) were performed on the basis of density functional theory with the B3LYP [46, 47] functional and the 6-311G (d,p) [48, 49] basis set in the gas phase. The excited state geometries were

Table 1 Polarity parameters of organic solvents

Solvent	Δf	E_{T}^{N}
Cyclohexane	0.002	0.01
Hexane	0.001	0.01
Benzene	0.003	0.11
Toluene	0.014	0.10
Chloroform	0.150	0.26
THF	0.210	0.21
Propanol-1	0.270	0.62
Ethanol	0.290	0.65
DMF	0.280	0.40

Δf is empirical Lippert parameter [42], E_{T}^{N} is normalized Dimroth-Reichardt parameter [44].

determined by means of TD-DFT with the CAM-B3LYP [50] functional and the 6-311G (d,p) basis set. Harmonic vibrational frequencies were computed at the same level of theory for S_0 state in order to characterize the stationary points as true minima, representing equilibrium structures on the potential energy surfaces. Frontier molecular orbitals (FMOs) diagrams were constructed on the optimized structures. The polarizable continuum model (PCM) applying dielectric constants of cyclohexane, hexane, benzene, toluene, chloroform, propan-1-ol, ethanol, DMF, and THF allowed to evaluate solvation effects.

Photostability

In order to determine the photostability of the 2,3;5,6-bis(cyclohexano)-BODIPY **1**, its solution in cyclohexane ($8.6 \cdot 10^{-6}$ mol/l) was subjected to the irradiation by UV light (mercury lamp DRL 250 with lighting power $W = 6.900$ mW/cm², irradiation by a light filter with a transmission of 365 nm). Electronic absorption spectra of the complex solution were recorded before and after irradiation at regular intervals (60 min). Depending on the irradiation time, the absorption at the maximum 546 nm of the characteristic band of EAS of 2,3;5,6-bis(cyclohexano)-BODIPY

1 was monitored. The relative absorption intensity (D/D_0) was calculated as the ratio of the absorption intensities at the maximum of the characteristic band of EAS after and before each irradiation.

The half-life ($\tau_{1/2}$) of the complex was determined from the $D/D_0 = f(t)$ dependence, as the irradiation time at which the optical density at the intense band maximum of the electronic absorption spectrum of the complex solution was decreased by 2.

Rate constant of the photodestruction as determined according to the following equations: $\ln(D_0/D_t) = kt$, where D_0 is the absorbance in maximum wavelength before the irradiation, D_t is the absorbance in maximum wavelength after the irradiation. The slope, k , is the rate of the photodestruction.

Results and Discussion

¹H NMR Spectra Description

In this section, the ¹H NMR spectra of complex **1** and 2,3;5,6-bis(cyclohexano)dipyrrromethene hydrobromide are compared to confirm the structure of the synthesized

Fig. 2 ¹H NMR spectra of 2,3;5,6-bis(cyclohexano)-dipyrrromethene hydrobromide (**a**) and 2,3;5,6-bis(cyclohexano)-BODIPY **1** (**b**)

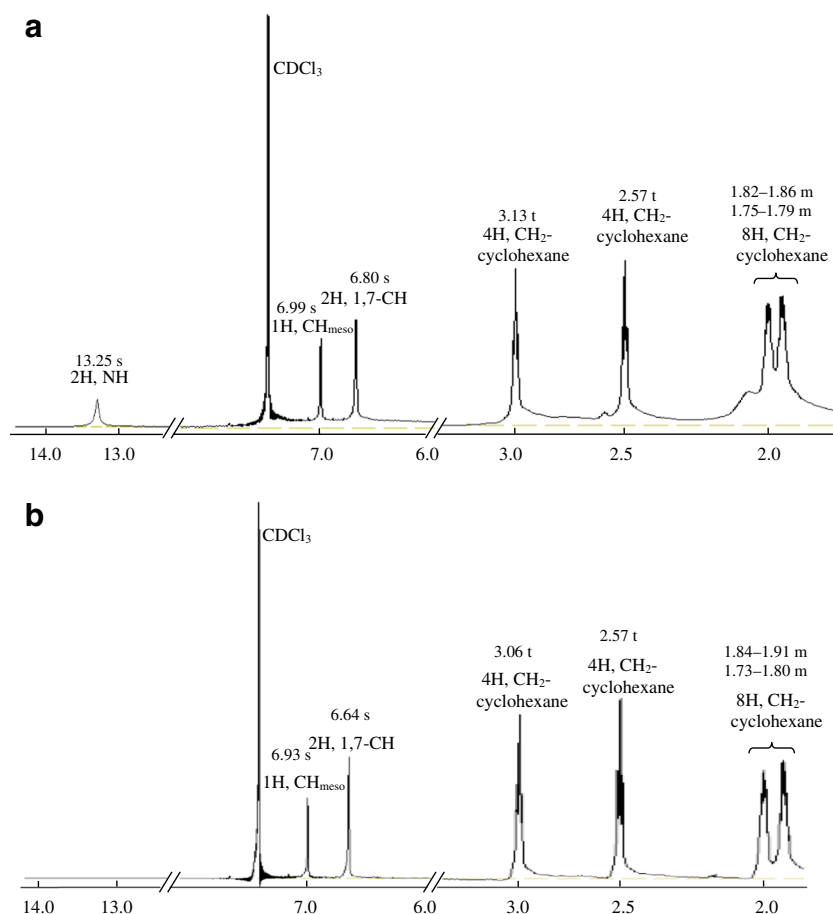


Table 2 Spectral-luminescent characteristics of 2,3;5,6-bis(cyclohexano)-BODIPY **1**

Solvent	Spectral-luminescent characteristics								
	$\lambda_{\text{max}}^{\text{abs}}$, nm $S_0 \rightarrow S_1$ $S_0 \rightarrow S_{1(\text{sh})}$ $S_0 \rightarrow S_2$	A , l/mol·cm $S_0 \rightarrow S_1$ $S_0 \rightarrow S_{1(\text{sh})}$ $S_0 \rightarrow S_2$	$\nu_{\text{max}}^{\text{abs}}$, cm^{-1} $S_0 \rightarrow S_1$	FWHM cm^{-1} Abs	$\lambda_{\text{max}}^{\text{fl}}$, nm $S_1 \rightarrow S_0$	$\nu_{\text{max}}^{\text{fl}}$, cm^{-1} $S_1 \rightarrow S_0$	FWHM cm^{-1} FL	$\Delta\lambda_{\text{St}}$, nm	$\Delta\nu_{\text{St}}$, cm^{-1}
C_6H_{12}	546	84,587	18,315	541	554	18,051	707	8	265
	517	30,086							
	366–371	7087							
C_6H_{14}	545	95,948	18,349	580	555	18,018	766	10	331
	516	32,586							
	364–371	7483							
C_6H_6	548	82,205	18,248	706	559	17,889	757	11	359
	521	31,285							
	366–370	7513							
$\text{C}_6\text{H}_5\text{-CH}_3$	548	79,834	18,248	709	558	17,921	760	10	327
	521	29,511							
	366–371	6795							
CHCl_3	549	79,130	18,215	741	559	17,889	727	10	326
	521	30,373							
	364–370	7470							
THF	544	76,640	18,382	827	556	17,986	766	12	396
	517	31,305							
	362–369	7261							
PrOH-1	544	77,921	18,382	863	554	18,051	678	10	332
	517	32,347							
	360–369	8133							
EtOH	543	74,033	18,416	866	553	18,083	712	10	333
	516	31,977							
	362–368	7976							
DMF	543	66,135	18,416	896	555	18,018	738	12	398
	519	29,465							
	364–371	7771							

$\lambda_{\text{max}}^{\text{abs}}$ is maximum $S_0 \rightarrow S_1$ and $S_0 \rightarrow S_2$ bands of absorption (nm); sh is shoulder, which is attributed to vibrational component of $S_0 \rightarrow S_1$ band; A is absorption molar coefficient (l/mol·cm); $\lambda_{\text{max}}^{\text{fl}}$ is $S_1 \rightarrow S_0$ band maximum in the fluorescence spectrum (nm); FWHM is full width at half maximum in the electronic absorption and fluorescence spectrum (cm^{-1}); $\Delta\lambda_{\text{St}}$ (nm) and $\Delta\nu_{\text{St}}$ (cm^{-1}) is Stokes shift

Table 3 Spectral-luminescent characteristics of 2,3;5,6-bis(cyclohexano)-BODIPY **1**

Solvent	Spectral-luminescent characteristics			
	ϕ $S_1 \rightarrow S_0$ (λ_{ex} , nm)	k_{rad} , s^{-1} ($\cdot 10^7 \text{ s}^{-1}$)	k_{nr} , s^{-1} ($\cdot 10^7 \text{ s}^{-1}$)	τ , ns
C_6H_{12}	0.92 (495)	5.01	0.39	18.44
C_6H_{14}	0.83 (495)	6.11	1.24	13.61
C_6H_6	~1.00 (495)	6.28	0	15.92
$\text{C}_6\text{H}_5\text{-CH}_3$	0.97 (495)	6.41	0.21	15.10
CHCl_3	0.97 (495)	6.34	0.20	15.29
THF	0.89 (500)	6.98	0.85	12.77
PrOH-1	0.98 (495)	7.41	0.17	13.19
EtOH	0.92 (500)	7.08	0.62	12.98
DMF	0.82 (495)	6.55	1.43	12.53

ϕ is fluorescence quantum yield; k_{rad} is rate constant of radiative process ($\cdot 10^7 \text{ s}^{-1}$); k_{nr} is rate constant of non-radiative process ($\cdot 10^7 \text{ s}^{-1}$); τ is fluorescence lifetime (ns)

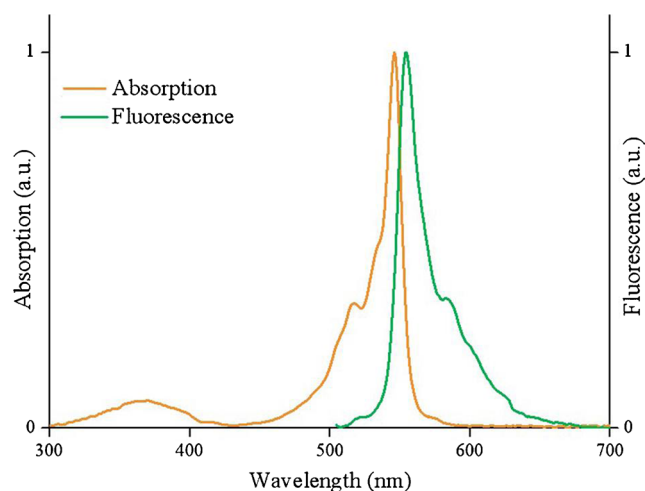
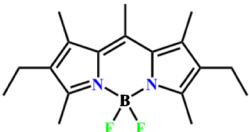
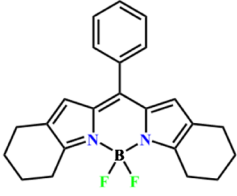
**Fig. 3** Normalized electronic absorption and emission spectra of 2,3;5,6-bis(cyclohexano)-BODIPY **1** in cyclohexane

Table 4 BODIPYs 2–8 with aliphatic acyclic and cyclic substituents

BODIPY 2–4 with aliphatic acyclic substituents				
BDP				
No	2 ^[13]	3 ^[13]	4 ^[55]	
ϕ	0.80 (EtOH)	0.70 (EtOH)	0.91 (EtOH)	
$\lambda_{\max}^{\text{abs}}$	505 nm	517 nm	529 nm	
$\lambda_{\max}^{\text{fl}}$	516 nm	546 nm	540 nm	
BODIPY 5–8 with aliphatic cyclic substituents				
BDP				
No	5 ^[33, 56]	6 ^[13]	7 ^[32]	8 ^[13]
ϕ	0.69 (MeCN), 0.78 (MeOH), 0.92 (THF), 0.86 (toluene)	0.84 (EtOH)	–	0.81 (EtOH)
$\lambda_{\max}^{\text{abs}}$	514 nm (MeCN), 515 nm (MeOH), 517 nm (THF), 523 nm (toluene)	535 nm	–	512 nm
$\lambda_{\max}^{\text{fl}}$	527 nm (MeCN), 527 nm (MeOH), 529 nm (THF), 534 nm (toluene)	560 nm	–	535 nm

BODIPY 1. The ^1H NMR spectrum of ligand (Fig. 2a) contains several peaks corresponding to the chemical shifts of protons of different groups. The signals of protons of six-membered aliphatic rings are in the region of 1.75–3.13 ppm. The bands in the form of singlets at 6.99 and 6.80 ppm, respectively, refer to the proton signals of a methine *meso*-spacer and two symmetrically arranged protons at the 1,7-positions of pyrroles. The pyrrole and pyrrolenine N–H protons in the form of singlet were located at 13.26 ppm.

From ^1H NMR of complex **1** (Fig. 2b), the disappearance of the signal at 13.25 ppm for N–H protons, and also shifting of proton signals to a strong field: the protons of cyclohexane

groups in the region of 1.73–3.06 ppm, protons of the *meso*-spacer and 1,7-protons of the pyrrole rings, respectively, at 6.93 and 6.64 ppm confirms the formation of complex **1**. The proton signals of individual groups in the ^1H NMR spectrum of the obtained complex retain a high characteristic nature and do not overlap (Fig. 2).

The observed regularities of the arrangement of the signals of individual proton groups in ^1H NMR spectrum of BODIPY **1** correspond to those of other structurally related BODIPYs and other dipyrromethene dyes [51–53].

Thus, unlike cyclohexano-substituted dipyrromethene, in the ^1H NMR spectrum of the aliphatic acyclic derivative, for

example, 4,4'-diethyl-3,3',5,5'-tetramethyldipyromethene hydrobromide, [53] the proton signal of NH groups was shifted to a stronger field by ~ 0.4 ppm ($\delta = 12.87$ ppm). Conversely, the proton signal of the methine *meso*-spacer was shifted to a weaker (by 0.05 ppm) field at 7.04 ppm. Signals of the protons of alkyl groups in the form of singlets, triplets and quartets are in the range 1.07–2.65 ppm. When complexing 4,4'-diethyl-3,3',5,5'-tetramethyldipyromethene

hydrobromide with boron(III), as in the case of BODIPY **1**, a strong-field shift of all proton signals is observed.

Spectral-Fluorescent Properties

Spectral-fluorescent characteristics of 2,3;5,6-bis(cyclohexano)-BODIPY **1** were obtained in a series of organic solvents of different polarity (Tables 2 and 3).

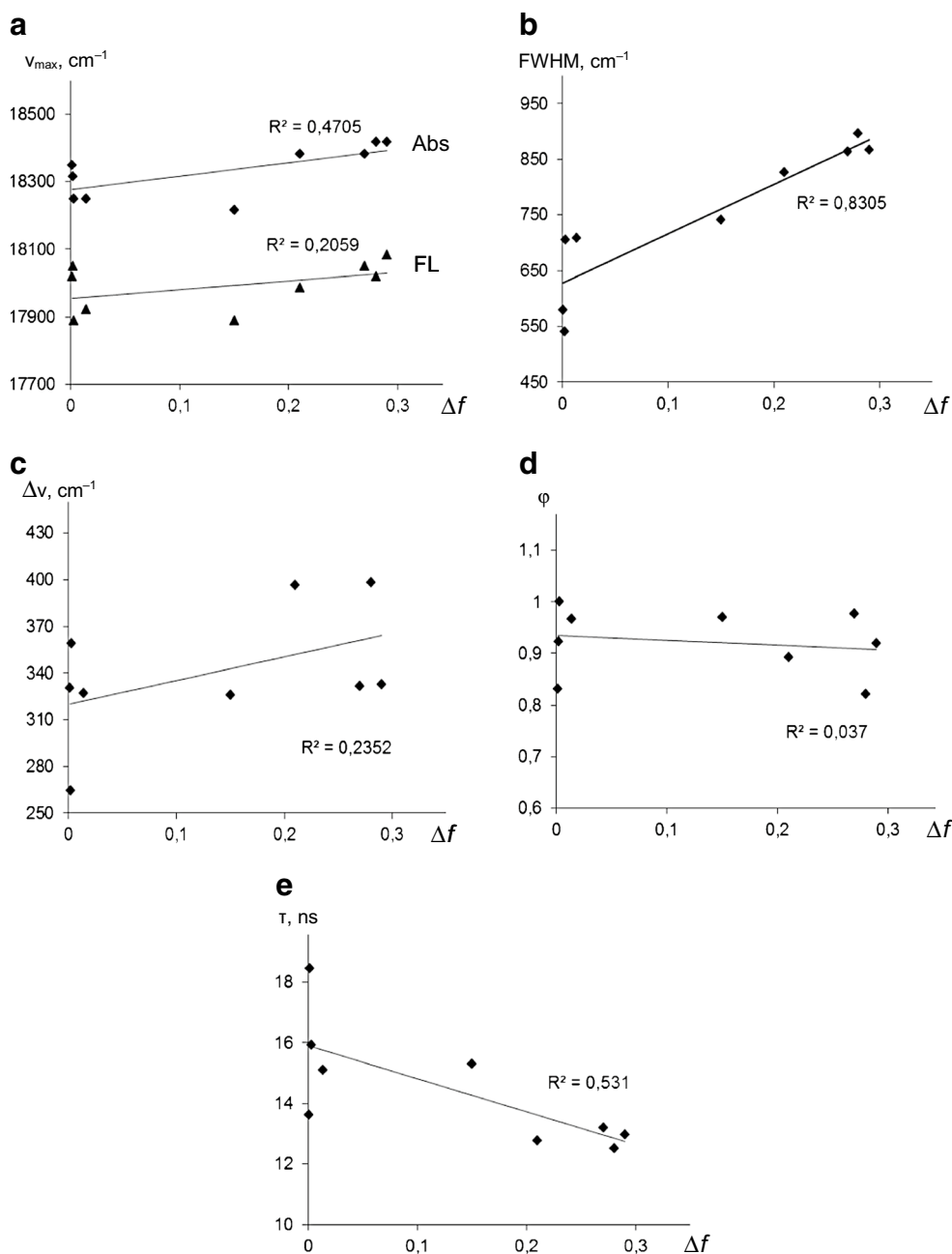
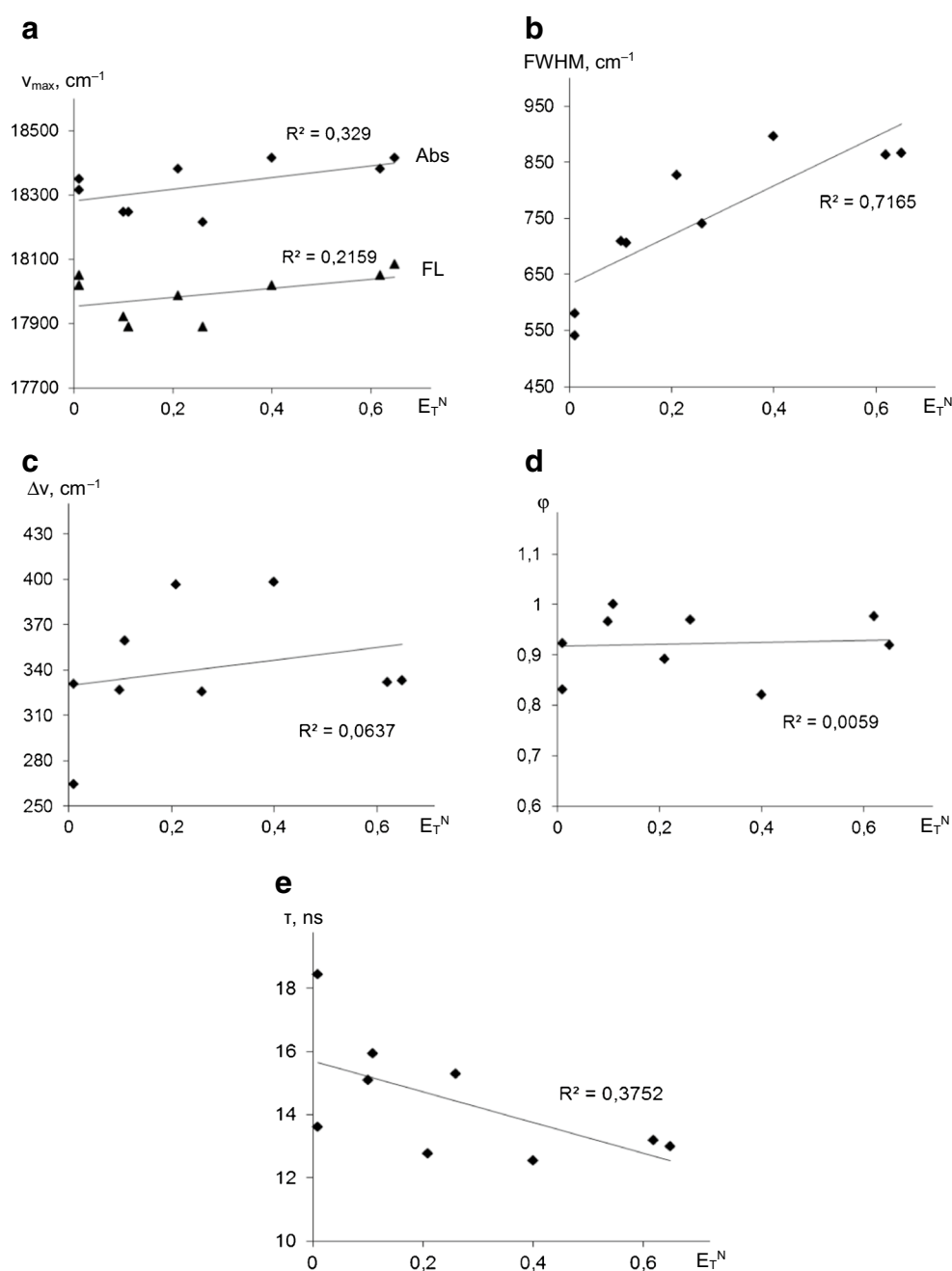


Fig. 4 Dependencies of spectral characteristics of BODIPY **1** on Lippert parameter: $\nu_{\max} = f(\Delta f)$, **a**; $\text{FWHM} = f(\Delta f)$, **b**; $\Delta\nu = f(E_T^N)$, **c**; $\phi = f(\Delta f)$, **d**; $\tau = f(\Delta f)$, **e**

Fig. 5 Dependencies of spectral characteristics of BODIPY **1** on Dimroth-Reichardt parameter: $\nu_{\max} = f(E_T^N)$, **a**; $\text{FWHM} = f(E_T^N)$, **b**; $\Delta\nu = f(E_T^N)$, **c**; $\varphi = f(E_T^N)$, **d**; $\tau = f(E_T^N)$, **e**



In the general case, the electronic absorption spectrum of **1** is similar in character to the EAS of other structurally related compounds and is typical for dyes of the 4,4-difluoro-3a,4a-diaza-s-indacene family. The absorption spectrum of **1** in organic solvents contains one intense long-wavelength band in the region with a maximum of 543–549 nm due to the $S_0 \rightarrow S_1$ electron transition (Fig. 3). The molar absorption coefficient of the $S_0 \rightarrow S_1$ band is 66,135–95,948 L/mol·cm (Table 2) and is comparable to that of other structurally related BODIPYs.

The shoulder at 516–521 nm is recorded on the left slope of the first band, which is attributed to the vibrational

transition of the $S_0 \rightarrow S_1$ band [54]. The second low-intensity broadened $S_0 \rightarrow S_2$ band is located in the near-UV region at 360–371 nm.

The fluorescence spectra of 2,3;5,6-bis(cyclohexano)-BODIPY are a mirror image of their EASs with a Stokes shift of 8–12 nm (Fig. 3). The fluorescence band of the complex is recorded in the region with a maximum ($\lambda_{\max}^{\text{fl}}$) at 554–559 nm (excitation at 495–505 nm). The fluorescence quantum yield (φ) of 2,3;5,6-bis(cyclohexano)-BODIPY **1** reaches 0.82–1.00 (Table 3) and is comparable with the values for many other alkyl-substituted BODIPYs [55].

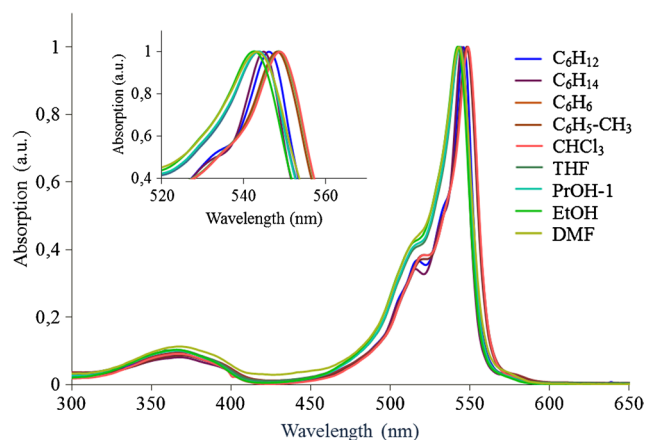


Fig. 6 Normalized electronic absorption spectra of 2,3,5,6-bis(cyclohexano)-BODIPY **1** in organic solvents; fragment of spectra in the enlarged scale (insert)

The constants of radiative (k_{rad}) and nonradiative (k_{nr}) processes for BODIPY **1** were $4.63 \cdot 10^7$ – $7.41 \cdot 10^7$ s $^{-1}$ and 0 – $1.43 \cdot 10^7$ s $^{-1}$, respectively, depending on the solvent nature (Table 3). The fluorophore lifetime (Table 3) in the excited state reaches values from 12.53 ns in DMF to 18.44 ns in cyclohexane.

It should be noted, that the currently obtained BODIPY derivatives with aliphatic rings, annelated to pyrrole fragments, (Table 4, compounds **1**, **5**–**8**) are more conformationally restricted, than BODIPYs containing acyclic aliphatic substituents (Table 4, compounds **2**–**4**) [13, 32, 33, 55, 56].

Formally, conjugated bonds systems in BODIPY core with acyclic (compounds **2**–**4**) and cyclic (compounds **1**, **5**–**8**) aliphatic substituents are similar. The molar absorption coefficients of these two groups of complexes are in the range 70,000–90,000 L/mol·cm.

Compared with alkylated BODIPY **4**, the “closing” of alkyl substituents in the cyclohexyl rings gives a significant bathochromic shift of the $\lambda_{\text{max}}^{\text{abs}}$ (up to 6–16 nm) and $\lambda_{\text{max}}^{\text{fl}}$ (12–21 nm) in the spectra of the bis(cyclohexano)-BODIPY **1** and **6** solutions, while maintaining a high (up to ~100%) fluorescence quantum yield (Tables 3 and 4) [13, 34]. Moreover, the largest red shift is observed in the emission spectra. The authors of Ref [35], explain such a red shift by the influence of cyclohexyl fragments, which give greater rigidity to the BODIPY molecule.

In addition, the spectral-luminescent properties of bis(cyclohexano)-BODIPYs depend on the site of attachment of the aliphatic rings and, as well as the number of carbon atoms in the aliphatic ring. For example, the absorption and emission bands maxima of compound **8**, containing aliphatic 5-membered rings in the 1,2 and 6,7-positions of BODIPY pyrroles, correspond to the same

spectral range as for BODIPY **2**–**4** with acyclic aliphatic substituents on the periphery of pyrrole rings.

Unfortunately, data on the spectral characteristics of BODIPY **7** are not available in the original article [32].

Solvatochromism

Analysis of spectral-luminescent characteristics of 2,3,5,6-bis(cyclohexano)-BODIPY **1** in nine different

Table 5 Calculated spectroscopic characteristics and FMOs energies of BODIPY **1**, calculated in solvents

Solvent	Transitions	f	E_{0-0} , eV	λ , nm
Cyclohexane	H–L	0.808	2.704	459
	H-1–L	0.131	3.932	315
	H-3–L	0.172	5.341	232
	H–L+1	0.145	6.207	200
	H–L+2	0.164	6.736	184
Hexane	H–L	0.797	2.718	456
	H-1–L	0.132	3.935	315
	H-3–L	0.167	5.348	231
	H–L+1	0.141	6.211	200
	H–L+2	0.159	6.738	184
Toluene	H–L	0.821	2.687	461
	H-1–L	0.130	3.931	315
	H-3–L	0.179	5.333	232
	H–L+1	0.149	6.201	200
	H–L+2	0.170	6.734	184
Benzene	H–L	0.823	2.686	462
	H-1–L	0.130	3.930	315
	H-3–L	0.180	5.332	233
	H–L+1	0.149	6.201	200
	H–L+2	0.171	6.733	184
THF	H–L	0.796	2.719	456
	H-1–L	0.136	3.954	313
	H-3–L	0.168	5.354	233
	H–L+1	0.120	6.201	200
	H–L+2	0.146	6.748	184
CHCl ₃	H–L	0.807	2.706	458
	H-1–L	0.134	3.946	314
	H-3–L	0.173	5.346	232
	H–L+1	0.139	6.201	200
	H–L+2	0.159	6.743	184
DMF	H–L	0.799	2.716	456
	H-1–L	0.137	3.958	313
	H-3–L	0.170	5.354	232
	H–L+1	0.097	6.196	200
	H–L+2	0.142	6.749	184
propan-1-ol	H–L	0.789	2.728	454
	H-1–L	0.138	3.960	313
	H-3–L	0.165	5.360	231
	H–L+1	0.068	6.199	200
	H–L+2	0.132	6.751	184
ethanol	H–L	0.783	2.735	453
	H-1–L	0.139	3.963	313
	H-3–L	0.162	5.364	231
	H–L+1	0.081	6.199	200
	H–L+2	0.124	6.753	184

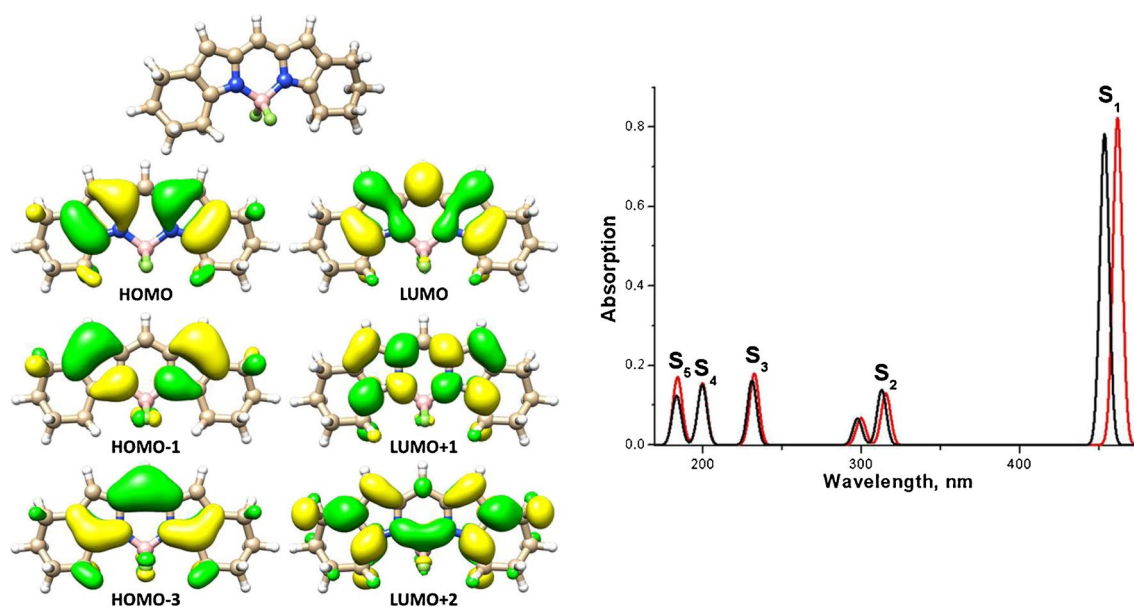


Fig. 7 The optimized geometry and FMOs (a) and theoretical UV/Vis spectra (ethanol (black) and benzene (red)) of BODIPY 1

organic solvents (Tables 2 and 3) allowed to study its solvatochromism (dependence of its spectral properties on solvent). The maxima positions of the $S_0 \rightarrow S_1$ band in the electronic absorption and fluorescence spectra, the width of the bands of spectra, the values of the Stokes shifts, and the fluorescence quantum yield of compound 1 were analyzed using solvatochromic parameters (Table 1). In Figs. 4 and 5 the dependences of the spectral characteristics on the Lippert and Dimroth–Reichardt parameters are presented.

The effect of the medium nature in the EAS is manifested in the red (2–6 nm) shift of the intense band (Fig. 6)

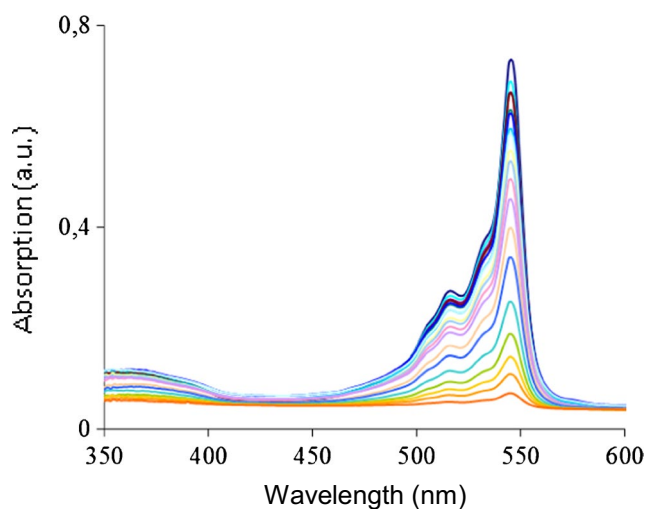


Fig. 8 Changes in the electronic absorption spectra of complex 1 in cyclohexane at irradiation by UV light (365 nm)

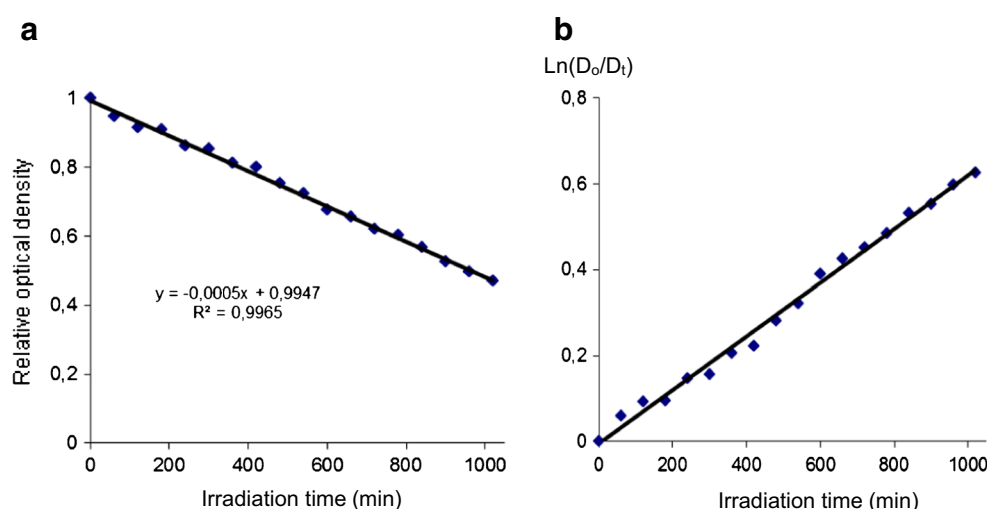
and the increase in the extinction coefficient (by $\sim 30,000$ l/mol·cm) upon transition from the group of polar (THF, alcohols, DMF) to the group of nonpolar (cyclohexane, hexane) solvents (Table 2).

A similar tendency of a red shift of the maximum position $\lambda_{\text{max}}^{\text{fl}}$ of the band with a decreasing polarity of the solvent is not observed in the fluorescence spectra (Table 2).

However, in the electronic absorption and fluorescence spectra of the complex in weakly polar chloroform and non-polar aromatic solvents (benzene, toluene) in comparison with nonpolar saturated hydrocarbons (cyclohexane, hexane) and polar (THF, propanol-1, ethanol, DMF) solvents, a red shift (up to 5–6 nm) of the $S_0 \rightarrow S_1$ band maximum is observed (Table 2). This can be caused by the specific solvation of the fluorine and nitrogen atoms of BODIPY by protons of a chloroform molecule or by π - π -stacking interactions of π -systems of dipyrromethene molecules and aromatic solvents. This behavior is typical for other BODIPYs [9, 55].

Narrowing of the intense band of the electronic absorption spectrum is observed in the transition from polar to nonpolar media (Table 2). The FWHM values for the complex in DMF are 896 cm^{-1} and decrease by more than 350 cm^{-1} in cyclohexane (541 cm^{-1}). In Figs. 4b and 5b show the dependencies $\text{FWHM} = f(\Delta f)$ and $\text{FWHM} = f(E_T^N)$ with the correlation coefficients $R^2 = 0.8303$ and 0.7165 , respectively. The FWHM values in the fluorescence spectra do not correlate with the medium polarity (Table 2) and vary in the range 678 – 766 cm^{-1} .

Fig. 9 Dependence of the relative optical density on the UV irradiation time (a) and logarithmic dependence of the relative optical density $\ln(D_0/D_t)$ on the UV irradiation time (b)



The Stokes shift value does not correlate with the polarity parameters of the solvents. The correlation coefficients for these dependences (Figs. 4c and 5c) do not exceed $R^2 = 0.2352$.

The fluorescence of complex **1** is weakly sensitive to the medium polarity. Almost in all the studied solvents (cyclohexane, benzene, toluene, THF, chloroform, alcohols), the values of ϕ vary from 0.89 to ~ 1 (Figs. 4d, 5d; Table 3). A decrease in the fluorescence quantum yield (by $\sim 15\%$) is observed only in hexane ($\phi = 0.83$) and DMF ($\phi = 0.82$). The lack of fluorescence selectivity to the medium polarity distinguishes BODIPY **1**, as well as most other BODIPY derivatives [57], from Zn(II) complexes with dipyrromethenes [58, 59].

The fluorophore lifetime (Table 3) in the excited state reaches 18.44 ns in nonpolar cyclohexane. With an increase in the medium polarity parameter, the lifetime is slightly decreased ($\tau = 12.53$ ns in DMF). The correlation coefficients for the dependences of the lifetime on the polarity parameters in Figs. 4e and 5e reach 0.531 and 0.372.

Quantum Chemical Calculations

To better understand the results of the spectroscopic measurements, quantum chemical calculations were carried out. The optimized structure of isolated BODIPY **1** obtained from DFT calculations using the B3LYP/6–311G (d,p) method is shown in Fig. 7. Computed absorption energies for the excited states of BODIPY **1** are shown in Table 5. The absorption energies have been calculated using the CAM-B3LYP/6–311G(d,p) and cyclohexane, hexane, toluene, benzene, THF, CHCl_3 , DMF, propan-1-ol, ethanol as a solvent.

The computed absorption spectra of BODIPY **1** show five bands of different intensity caused by the S_0 - S_n electronic transitions (Table 5; Fig. 7b). The most intense

S_0 - S_1 absorption band has a maximum in the range of 462–453 nm (depending on the solvent), and caused by the HOMO–LUMO transition. In the range of 313–213 nm there are the bands belonging to S_0 - S_2 , S_0 - S_3 electronic transition (HOMO-1–LUMO, HOMO-3–LUMO, respectively); in the range of 200–184 nm the S_0 - S_4 and S_0 - S_5 bands (HOMO–LUMO + 1, HOMO–LUMO + 2) are registered. All electronic transitions are caused by the redistribution of the electron density in the BODIPY **1** core.

The intense S_0 - S_1 absorption band is most sensitive to the solvent polarity (Fig. 7b). This band is shifted to the red region at the transition from polar to non-polar solvents (Fig. 7b; Table 5). Also, the pattern of increasing the energy gap (E_{0-0}) of HOMO–LUMO transition is observed in a series of solvents: benzene – toluene – cyclohexane – CHCl_3 – DMF – hexane – THF – propan-1-ol – ethanol (Table 5). Thus, improving spectral-luminescent properties of BODIPY **1** can be expected when replacing non-polar to polar solvents.

Photochemical Stability

The spectral-luminescent properties of BODIPYs in organic solvents remain unchanged for several months of their storage in the light. On the other hand, studies [59, 60] show that the molecular structure of dipyrromethene dyes, including BODIPY, is more sensitive to UV radiation.

The change in the EAS of a complex **1** solution in cyclohexane under UV irradiation is shown in Fig. 8. Photodestruction of complex **1** in the process of UV irradiation (365 nm) is accompanied by a decrease in the absorption of the characteristic $S_0 \rightarrow S_1$ band of the complex in the visible region of the spectrum (Fig. 8).

With UV irradiation, the $S_0 \rightarrow S_1$ band of EAS of complex **1** disappears completely only after about 30 h of irradiation

of the solution. From the data, shown in Fig. 9a, the half-life ($\tau_{1/2}$) under the action of UV-irradiation was 980 min. The rate constant of the photodestruction of compound **1** under the UV irradiation of the solution, determined from the dependence in Fig. 9b, was $6.75 \cdot 10^{-4}$ mol/min.

The value of the rate constant of the destruction of complex **1** is comparable to the data for structurally related *meso*-phenyl substituted BODIPYs [60, 61].

Conclusions

Thus, the study of the properties of 2,3;5,6-bis(cyclohexano)-BODIPY **1** showed that the dye has intense chromophore properties ($\lambda_{\max} = 543\text{--}549$ nm, $A = 66,135\text{--}95,948$ L/mol-cm), comparable to alkyl-substituted BODIPYs dyes. The 2,3;5,6-bis(cyclohexano)-BODIPY is an effective fluorophore with a quantum yield of 82–100%. The fluorescence quantum yield of the dye is weakly depends on the medium polarity. Structure of 2,3;5,6-bis(cyclohexano)-BODIPY is stable in visible light and more sensitive to UV irradiation. With UV irradiation (365 nm), the complex undergoes complete destruction with a half-life of 980 min and a rate constant of $6.75 \cdot 10^{-4}$ mol/min.

Acknowledgements The reported study was funded by RFBR according to the research project No. 16-33-00611 mol_a and 16-33-00852 mol_a. We are grateful to the Interdisciplinary Supercomputer Center of the Russian Academy of Sciences (Moscow) for providing MBC 100 K cluster resources.

References

- Banuelos J (2016) BODIPY dye, the most versatile fluorophore ever? Chem Rec 16:335–348. <https://doi.org/10.1002/tcr.201500238>
- Treibs A, Kreuzer FH (1968) Difluoroboryl-Komplexe von Di- und tripyrrylmethenen. Eur J Org Chem 718:208–223. <https://doi.org/10.1002/jlac.19687180119>
- Shah M, Thangaraj K, Soong ML, Wolford L, Boyer JH, Politzer I, Pavlopoulos TG (1990) Pyromethene-BF₂ complexes as laser dyes: 1. Heteroat Chem 1: 389–399. <https://doi.org/10.1002/hc.520010507>
- Guggenheimer SC, Boyer JH, Thangaraj K, Shah M, Soong ML, Pavlopoulos TG (1993) Efficient laser action from two cw laser-pumped pyromethene-BF₂ complexes. Appl Opt 32:3942–3943. <https://doi.org/10.1364/AO.32.003942>
- Boyer JH, Haag AM, Sathyamoorthi G, Soong ML, Thangaraj K (1993) Pyromethene-BF₂ complexes as laser dyes: 2. Heteroat Chem 4:39–43. <https://doi.org/10.1002/hc.520040107>
- Yariv E, Schultheiss S, Saraidarov T, Reisfeld R (2001) Efficiency and photostability of dye-doped solid-state lasers in different hosts. Opt Mater 16:29–38. [https://doi.org/10.1016/S0925-3467\(00\)00056-2](https://doi.org/10.1016/S0925-3467(00)00056-2)
- Lai RY, Bard AJ (2003) Electrogenerated Chemiluminescence 71. Photophysical, electrochemical, and electrogenerated chemiluminescent properties of selected dipyrromethene – BF₂ dyes. J Phys Chem B 107:5036–5042. <https://doi.org/10.1021/jp034578h>
- Lopez Arbeloa F, Banuelos J, Martinez V, Arbeloa T, Lopez Arbeloa I (2005) Structural, photophysical and lasing properties of pyromethene dyes. Int Rev Phys Chem 24:339–374. <https://doi.org/10.1080/01442350500270551>
- Qin W, Baruah M, Auweraer M, Schryver F, Boens N (2005) Photophysical properties of borondipyrromethene analogues in solution. J Phys Chem A 109:7371–7384. <https://doi.org/10.1021/jp052626n>
- Garcia O, Sastre R, del Agua D, Costela A, Garcia-Moreno I, Lopez Arbeloa F, Banuelos Prieto J, Lopez Arbeloa I (2007) Laser and physical properties of BODIPY chromophores in new fluorinated polymeric materials. J Phys Chem C 111:1508–1516. <https://doi.org/10.1021/jp065080t>
- Susdorf T, del Agua D, Tyagi A, Penzkofer A, Ggarcia O, Sastre R, Costela A, Garcia-Moreno I (2007) Photophysical characterization of pyromethene 597 laser dye in silicon-containing organic matrices. Appl Phys B 86:537–545. <https://doi.org/10.1007/s00340-006-2439-z>
- Thorat KG, Kamble P, Mallah R, Ray AK, Sekar N., and Theory TD-DFT. (2015) Congeners of Pyromethene-567 dye: perspectives from synthesis, photophysics, photostability, laser. J Org Chem 80:6152–6164. <https://doi.org/10.1021/acs.joc.5b00654>
- Loudet A, Burgess K (2007) BODIPY dyes and their derivatives: syntheses and spectroscopic properties. Chem Rev 107:4891–4932. <https://doi.org/10.1021/cr078381n>
- Ziessel R, Ulrich G, Harriman A (2007) The chemistry of BODIPY: a new El Dorado for fluorescence tools. New J Chem 31:496–501. <https://doi.org/10.1039/B617972J>
- Ulrich G, Ziessel R, Harriman A (2008) The chemistry of fluorescent biopoly dyes: versatility unsurpassed. Angew Chem Int Ed 47:1184–1201. <https://doi.org/10.1002/anie.200702070>
- Benstead M, Mehl GH, Boyle RW (2011) 4, 4'-Difluoro-4-bora-3a, 4a-diaza-s-indacenes (BODIPYs) as components of novel light active materials. Tetrahedron 67:3573–3601. <https://doi.org/10.1016/j.tet.2011.03.028>
- Boens N, Leen V, Dehaen W (2012) Fluorescent indicators based on BODIPY. Chem Soc Rev 41:1130–1172. <https://doi.org/10.1039/C1CS15132K>
- Zhu S, Zhang J, Janjanam J, Vegesna G, Luo F-T, Tiwari A, Liu H (2013) Highly water-soluble BODIPY-based fluorescent probes for sensitive fluorescent sensing of zinc(II). J Mater Chem B 1:1722–1728. <https://doi.org/10.1039/C3TB00249G>
- Zhao C, Zhang Y, Feng P, Cao J (2012) Development of a borondipyrromethene-based Zn²⁺ fluorescent probe: solvent effects on modulation sensing ability. Dalton Trans 41:831–838. <https://doi.org/10.1039/C1DT10797F>
- Peters C, Billich A, Ghobrial M, Hogenauer K, Ullrich T, Nussbaumer P (2007) Synthesis of Borondipyrromethene (BODIPY)-labeled sphingosine derivatives by cross-metathesis reaction. J Org Chem 72:1842–1845. <https://doi.org/10.1021/jo062347b>
- Wang D, Fan J, Gao X, Wang B, Sun S, Peng X (2009) Carboxyl BODIPY dyes from bicarboxylic anhydrides: one-pot preparation, spectral properties, photostability, and biolabeling. J Org Chem 74:7675–7683. <https://doi.org/10.1021/jo901149y>
- Bergstrom F, Mikhalyov I, Hagglof P, Wortmann R, Ny T, Johansson LB-Å (2002) Dimers of dipyrrometheneboron difluoride (BODIPY) with light spectroscopic applications in chemistry and biology. J Am Chem Soc 124:196–204. <https://doi.org/10.1021/ja010983f>
- Kamkaew A, Lim SH, Lee HB, Kiew LV, Chung LY, Burgess K (2013) BODIPY dyes in photodynamic therapy. Chem Soc Rev 42:77–88. <https://doi.org/10.1039/C2CS35216H>

24. Awuah SG, You Y (2012) Boron dipyrromethene (BODIPY)-based photosensitizers for photodynamic therapy. *RSC Advances* 2:11169–11183. <https://doi.org/10.1039/C2RA21404K>
25. Wan CW, Burghart A, Chen J, Bergström F, Johansson LBA, Wolford MF, Kim TG, Topp MR, Hochtrasser RM, Burgess K (2003) Anthracene–BODIPY cassettes: syntheses and energy transfer. *Chem Eur J* 9: 4430–4441. <https://doi.org/10.1002/chem.200304754>
26. D'Souza F, Smith PM, Zandler ME, McCarty AL, Itou M, Araki Y, Ito O (2004) Energy transfer followed by electron transfer in a supramolecular triad composed of boron dipyrin, zinc porphyrin, and fullerene: a model for the photosynthetic antenna-reaction center complex. *J Am Chem Soc* 126:7898–7907. <https://doi.org/10.1021/ja030647u>
27. Ooyama Y, Hagiwara Y, Mizumo T, Harima Y, Ohshita J (2013) Photovoltaic performance of dye-sensitized solar cells based on D– π –A type BODIPY dye with two pyridyl groups. *New J Chem* 37:2479–2485. <https://doi.org/10.1039/C3NJ00456B>
28. Ooyama Y, Hagiwara Y, Mizumo T, Harima Y, Ohshita J (2013) Synthesis of diphenylamino-carbazole substituted BODIPY dyes and their photovoltaic performance in dye-sensitized solar cells. *RSC Adv* 3:18099–18106. <https://doi.org/10.1039/C3RA43577F>
29. Rezende L, Vaidergorn M, Moraes J, Emery F, Synthesis (2014) Photophysical properties and solvatochromism of meso-substituted tetramethyl BODIPY dyes. *J Fluoresc* 24:257–266. <https://doi.org/10.1007/s10895-013-1293-8>
30. Filatov MA, Lebedev AY, Mukhin SN, Vinogradov SA, Cheprakov AV (2010) π -extended dipyrins capable of highly fluorogenic complexation with metal ions. *J Am Chem Soc* 132:9552–9554. <https://doi.org/10.1021/ja102852v>
31. Gresser R, Hoyer A, Hummert M, Hartmann H, Leo K, Riede M (2011) Homoleptic Co(II), Ni(II), Cu(II), Zn(II) and Hg(II) complexes of bis-(phenyl)-diisindol-aza-methene. *Dalton Trans* 40:3476–3483. <https://doi.org/10.1039/C0DT01655A>
32. Melanson JA, Smithen DA, Cameron TS, Thompson A (2014) Microwave-assisted reduction of F-BODIPYs and dipyrins to generate dipyrromethanes. *Can J Chem* 92:688–694. <https://doi.org/10.1139/cjc-2013-0341>
33. Leen V, Braeken E, Luckermans K, Jackers C, Van der Auweraer M, Boens N, Dehaen W (2009) A versatile, modular synthesis of monofunctionalized BODIPY dyes. *Chem Commun* 4515–4517. <https://doi.org/10.1039/B906164A>
34. Wu L, Burgess K (2008) A new synthesis of symmetric boraindacene (BODIPY) dyes. *Chem Commun* 4933–4935. <https://doi.org/10.1039/B810503K>
35. Alekseeva AS, Tretiakova DS, Melnikova DN, Molotkovsky UIG, Boldyrev IA (2016) Novel fluorescent membrane probe 2,3;5,6-Bis(Cyclohexyl)-BODIPY-labeled phosphatidylcholine. *Russ J Bioorg Chem* 42:305–309. <https://doi.org/10.1134/S1068162016030031>
36. Gordon, Ford R (1976) *Sputnik Chimica*, Mir, Moscow
37. Riddick JA, Bunger WB, Sakano TK (1986) *Organic solvents: physical properties and methods of purification*
38. Khodov IA, Nikiforov MY, Alper GA, Mamardashvili GM, Mamardashvili NZ, Koifman OI (2015) Synthesis and spectroscopic characterization of Ru(II) and Sn(IV)-porphyrins supramolecular complexes. *J Mol Struct* 1081:426–430. <https://doi.org/10.1016/j.molstruc.2014.10.070>
39. Maltceva O, Mamardashvili G, Khodov I, Lazovskiy D, Khodova V, Krest'yaninov M, Mamardashvili N, Dehaen W (2017) Molecular recognition of nitrogen-containing bases by Zn[5,15-bis-(2,6-dodecyloxyphenyl)]porphyrin. *Supramol Chem* 29:360–369. <https://doi.org/10.1080/10610278.2016.1238473>
40. Fischer M, Georges J (1996) Fluorescence quantum yield of rhodamine 6G in ethanol as a function of concentration using thermal lens spectrometry. *Chem Phys Lett* 260:115–118. [https://doi.org/10.1016/0009-2614\(96\)00838-X](https://doi.org/10.1016/0009-2614(96)00838-X)
41. Wolfbeis OS (2008) *Standardization and quality assurance in fluorescence measurements techniques*. Springer Ser Fluoresc
42. Lakowicz JR (ed) (2013) *Principles of fluorescence spectroscopy*. Springer Science & Business Media
43. Terenin AN (1967) *Photonics of dye molecules*. Nauka, Leningrad
44. Reichardt C (1994) Solvatochromic dyes as solvent polarity indicators. *Chem Rev* 94:2319–2358. <https://doi.org/10.1002/chin.199509296>
45. Schmidt MW, Baldrige KK, Boatz JA, Elbert ST, Gordon MS, Jensen JH, Koseki S, Matsunaga N, Nguyen KA, Su S, Windus TL, Dupuis M, Montgomery JA (1993) General atomic and molecular electronic structure system. *J Comput Chem* 14:1347–1363. <https://doi.org/10.1002/jcc.540141112>
46. Becke AD (1993) A new mixing of Hartree–Fock and local density-functional theories. *J Chem Phys* 98:1372. <https://doi.org/10.1063/1.464304>
47. Lee C, Yang W, Parr RG (1988) Development of the Colle–Salvetti correlation-energy formula into a functional of the electron density. *Phys Rev B* 37:785–789. <https://doi.org/10.1103/PhysRevB.37.785>
48. McLean AD, Chandler GS (1980) Contracted Gaussian-basis sets for molecular calculations. 1. 2nd row atoms, Z = 11–18. *J Chem Phys* 72:5639–5648. <https://doi.org/10.1063/1.438980>
49. Raghavachari K, Binkley JS, Seeger R, Pople JA (1980) Self-consistent molecular orbital methods. 20. Basis set for correlated wave-functions. *J Chem Phys* 72:650–654. <https://doi.org/10.1063/1.438955>
50. Yanai T, Tew D, Handy N (2004) “A new hybrid exchange–correlation functional using the Coulomb-attenuating method (CAM-B3LYP)”. *Chem Phys Lett* 393:51–57. <https://doi.org/10.1016/j.cplett.2004.06.011>
51. Nuraneeva EN, Guseva GB, Antina EV, Kuznetsova RT, Berezin MB, V'yugin AI (2016) Synthesis, spectral luminescent properties, and photostability of monoiodo- and dibromo-substituted BF₂-dipyrinates. *Russ J Gen Chem* 86:840–847. <https://doi.org/10.1134/S1070363216040149>
52. Dudina NA, Berezin MB, Semeikin AS, Antina EV (2015) Difluoroborates of phenyl-substituted aza-dipyrromethenes: preparation, spectral properties, and stability in solution. *Russ J Gen Chem* 85:2739–2742. <https://doi.org/10.1134/S1070363215120130>
53. Wood TE, Berno B, Beshara CS, Thompson A (2006) ¹⁵N NMR chemical shifts for the identification of dipyrrolic structures. *J Org Chem* 71:2964–2971. <https://doi.org/10.1021/jo0524932>
54. Qin W, Baruah M, der Auweraer MV, De Schryver FC, Boens N (2005) Photophysical properties of borondipyrromethene analogues in solution. *J Phys Chem A* 109:7371–7384. <https://doi.org/10.1021/jp052626n>
55. Bumagina NA, Antina EV, Berezin MB, Kalyagin AA (2017) Influence of structural and solvation factors on the spectral-fluorescent properties of alkyl-substituted BODIPYs in solutions. *Spectrochim Acta A Mol Biomol Spectrosc* 173: 228–234. <https://doi.org/10.1016/j.saa.2016.09.026>
56. Leen V (2010) Synthesis and application of reactive BODIPY dyes. Doctoral Thesis. Katholieke Universiteit Leuven
57. Dias de Rezende LC, Vaidergorn MM, Moraes JCB, da Silva Emery F (2014) Synthesis, photophysical properties and solvatochromism of meso-substituted tetramethyl BODIPY dyes. *J Fluoresc* 24:257–266. <https://doi.org/10.1007/s10895-013-1293-8>
58. Nuraneeva EN, Guseva GB, Antina EV, Berezin MB, V'yugin AI (2016) Synthesis and luminescent properties of zinc(II) complexes with iodo- and bromosubstituted 2,2'-dipyrines. *J Luminesc* 170:248–254. <https://doi.org/10.1016/j.jlumin.2015.10.061>

59. Dudina NA, Nikonova AY, Antina EV, Berezin MB, Vyugin AI (2014) Synthesis, spectral-luminescent properties and photostability of Zn(II) complexes with dipyrrens modified at the periphery and at the meso-spacer. *Chem Heterocycl Compd* 49:1740–1747. <https://doi.org/10.1007/s10593-014-1426-2>
60. Cui A, Peng X, Fan J, Chen X, Wu Y, Guo B (2007) Synthesis, spectral properties and photostability of novel boron-dipyrromethene dyes. *J Photochem Photobiol A* 186:85–92. <https://doi.org/10.1016/j.jphotochem.2006.07.015>
61. Zhang S, Wu T, Fan J, Li Zh, Jiang N, Wang J, Dou B, Sun Sh, Song F, Peng X (2013) A BODIPY-based fluorescent dye for mitochondria in living cells, with low cytotoxicity and high photostability. *Org Biomol Chem* 11:555–558. <https://doi.org/10.1039/C2OB26911B>